**Fig. 3.** The generation of siRNA requires RNA-PII. (**A**) The wild-type and *m203* mutant RNAPII molecules both localize to the pericentromeric heterochromatin. ChIP analysis was performed with an antibody against the C-terminal domain of RNAPII (CTD) or an antibody to hemagglutinin (HA) as a negative control. The *dh* pericentromeric repeat, as well as the transcribed *leu1* gene, accumulated in immunoprecipitates obtained from both the wild-type and *rpb2-m203* extracts. In contrast, the gene-free upstream region of *ste11* gene, which is not transcribed in vegetative cells (*20*), did not accumulate. No signal was obtained from immunoprecipitates generated by the control anti-HA antibody. Relative amount of the PCR product is shown below each lane. ND, not determined. (**B**) Accumulation of transcripts derived from the *dh* repeat was determined with semiquantitative strand-specific reverse transcription–polymerase chain reaction (RT-PCR). Actin (*act1*) was used as a positive control. RNA samples subjected to first-strand cDNA synthesis without reverse transcriptase were used to discriminate genomic DNA contamination (−RT). for, forward strand; rev, reverse strand. (**C**) Mean signal intensities and standard deviation of three independent RT-PCR experiments as in (A) were plotted. Relative amounts of RT-PCR product from each mutant and the wild type are shown. *dh* transcripts are hardly detectable in the wild type, whereas both forward- and reverse-strand transcripts accumulated to high levels in the mutants. (**D**) Northern blot analysis of siRNA corresponding to the centromeric *dh* repeat. siRNAs spanning 22 to 26 nt are readily detected in the wild type. The siRNAs are lost in the Δ*dcr1* RNAi mutant, as well as *rpb2-m203* and the *rpb2-m203* Δ*dcr1* double mutant. Blots were reprobed for U6 snRNA as a loading control.
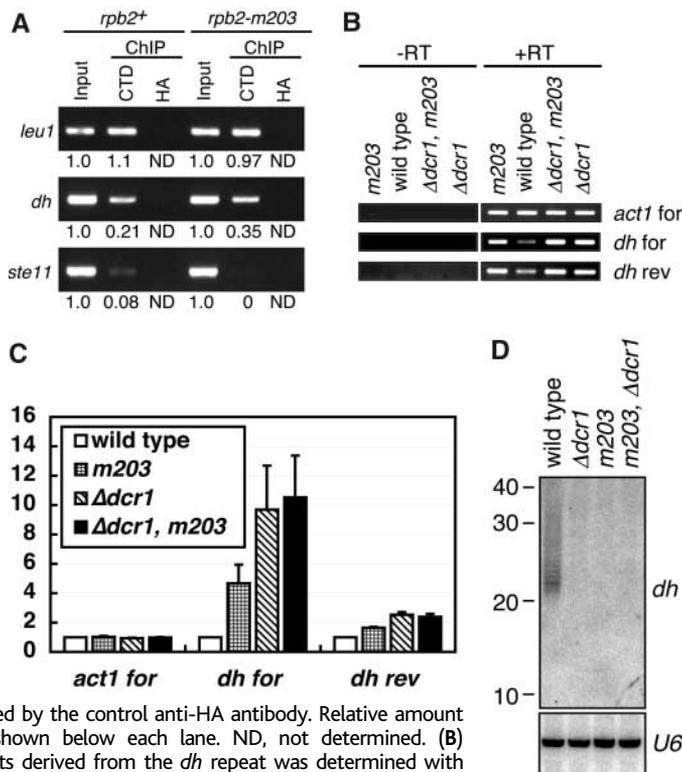


In *S. pombe* Rbp2, amino acid residue Asn[44] corresponds to Tyr[57] of *Saccharomyces cerevisiae* Rbp2 (Fig. 2). This residue is located on the surface of the protrusion domain of the RNAPII complex (*16, 17*). We speculate that conversion of Asn[44] to Tyr in *rpb2-m203* may diminish possible interactions between RNAPII and unknown factors required for generating siRNA. *S. cerevisiae* Rpb2 already has Tyr at this site, and the surrounding region is less conserved than the protein as a whole (Fig. 2). This may reflect the absence of RNAi machinery in budding yeast (*3*).

It has recently been shown that the two largest subunits of RNA polymerase IV (RNAPIV) in *Arabidopsis* are required for siRNA production from pericentromeric 5*S* ribosomal RNA gene clusters and *AtSN1* retroelements and contribute to heterochromatic organization (*18*). However, homologs of these subunits are found only in the plant kingdom (*18, 19*). Notably, the *rpb2-m203* mutation also has a highly specific effect on siRNA-directed heterochromatin formation in fission yeast, but unlike RNAPIV, Rpb2 is conserved in higher eukaryotes. It is likely that a role for RNAPII in RNAi is similarly conserved.

**References and Notes**
1. A. Verdel *et al.*, *Science* **303**, 672 (2004).
2. M. R. Motamedi *et al.*, *Cell* **119**, 789 (2004).
3. T. A. Volpe *et al.*, *Science* **297**, 1833 (2002).
4. M. Sadaie, T. Iida, T. Urano, J. Nakayama, *EMBO J.* **23**, 3825 (2004).
5. Z. Lippman *et al.*, *Nature* **430**, 471 (2004).
6. Materials and methods are available as supporting material on *Science* Online.
7. J. Nakayama, J. C. Rice, B. D. Strahl, C. D. Allis, S. I. Grewal, *Science* **292**, 110 (2001).
8. P. Bernard *et al.*, *Science* **294**, 2539 (2001).
9. N. Nonaka *et al.*, *Nat. Cell Biol.* **4**, 89 (2002).
10. M. Kawagishi-Kobayashi, M. Yamamoto, A. Ishihama, *Mol. Gen. Genet.* **250**, 1 (1996).
11. T. Tani, Y. Ohshima, *Nature* **337**, 87 (1989).
12. M. Hamada, A. L. Sakulich, S. B. Koduru, R. J. Maraia, *J. Biol. Chem.* **275**, 29076 (2000).
13. Y. Lee *et al.*, *EMBO J.* **23**, 4051 (2004).
14. D. A. Zorio, D. L. Bentley, *Exp. Cell Res.* **296**, 91 (2004).
15. R. A. Martienssen, *Nat. Genet.* **35**, 213 (2003).
16. J. Chen *et al.*, *Nucleic Acids Res.* **31**, 474 (2003).
17. K. J. Armache, S. Mitterweger, A. Meinhart, P. Cramer, *J. Biol. Chem.* **280**, 7131 (2005).
18. Y. Onodera *et al.*, *Cell* **120**, 613 (2005).
19. A. J. Herr, M. B. Jensen, T. Dalmay, B. Baulcombe, *Science* **308**, 118 (2005).
20. A. Sugimoto, Y. Iino, T. Maeda, Y. Watanabe, M. Yamamoto, *Genes Dev.* **5**, 1990 (1991).
21. We thank R. C. Allshire, S. I. S. Grewal, D. Q. Ding, and Y. Hiraoka for their gifts of strains and plasmids, and members of the Murakami laboratory and K. Tanaka for their support and discussions. D.B.G. is a U.S. Department of Energy–Energy Biosciences Research Fellow of the Life Sciences Research Foundation. This work is supported in part by a grant from NIH (R01-GM067014) to R.A.M., and by a Grant-in-aid for Scientific Research (B) to Y.M. from the Japan Society for the Promotion of Science.

# Apolipoprotein L-I Promotes Trypanosome Lysis by Forming Pores in Lysosomal Membranes

**David Pérez-Morga,[1]\* Benoit Vanhollebeke,[1]\* Françoise Paturiaux-Hanocq,[1] Derek P. Nolan,[2] Laurence Lins,[3] Fabrice Homblé,[4] Luc Vanhamme,[1] Patricia Tebabi,[1] Annette Pays,[1] Philippe Poelvoorde,[1] Alain Jacquet,[5] Robert Brasseur,[3] Etienne Pays[1]†**

Apolipoprotein L-I is the trypanolytic factor of human serum. Here we show that this protein contains a membrane pore-forming domain functionally similar to that of bacterial colicins, flanked by a membrane-addressing domain. In lipid bilayer membranes, apolipoprotein L-I formed anion channels. In *Trypanosoma brucei*, apolipoprotein L-I was targeted to the lysosomal membrane and triggered depolarization of this membrane, continuous influx of chloride, and subsequent osmotic swelling of the lysosome until the trypanosome lysed.

Apolipoprotein L-I (apoL-I) is a human-specific serum apolipoprotein bound to high-density lipoprotein (HDL) particles (*1–5*). This protein kills the African trypanosome *Trypanosoma brucei brucei*, except subspecies adapted to humans (*T. b. rhodesiense*, *T. b. gambiense*)
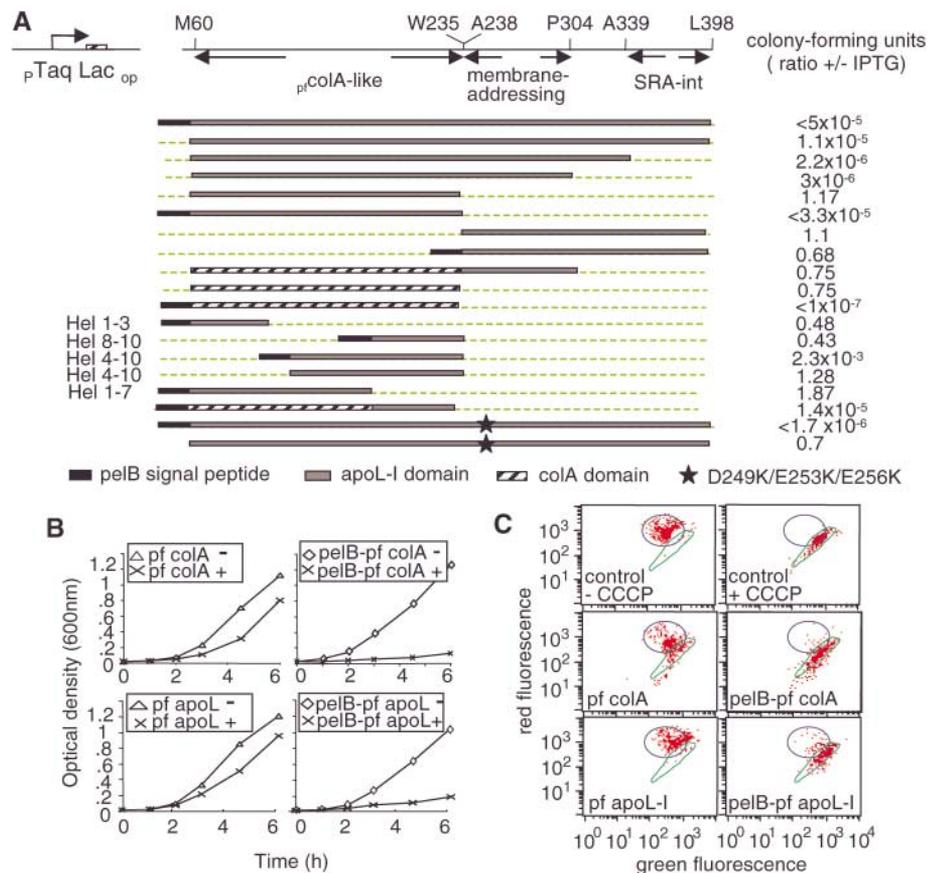
**Fig. 1.** Colicin-like activity of apoL-I. (**A**) Various pCT3-derived plasmids (*14*) were transfected into *E. coli* C600, and the bacterial plating efficiency was scored by comparing expression induction or not, after overnight incubation at 37°C. (**B**) Effect of the apoL-I and colA pf domains, flanked or not by pelB, on growth of *E. coli*. Expression of the two domains was induced (+) or not (−) by IPTG (isopropyl-β-D-thiogalactopyranoside). (**C**) Effect of the apoL-I and colA pf domains on the membrane potential of *E. coli*, as measured after 3 hours by flow cytometry with the DiOC$_2$ (3) probe. The ionophore CCCP (5 μM) was used to visualize the fluorescence shift linked to membrane depolarization.

(*5–7*). Trypanosome lysis results from uptake of apoL-I into the lysosome (*6*), and is thought to involve HDL receptor–mediated uptake of the lytic factor (*7–10*), which would lead to disruption of the lysosomal membrane following lipid peroxidation (*8*, *11*).

The C-terminal F342-L398 region of apoL-I, which interacts with the *T. b. rhodesiense* neutralizing protein SRA, is not required for trypanolytic activity (*6*). To define the

[1]Laboratory of Molecular Parasitology, IBMM, Université Libre de Bruxelles, 12, rue des Profs Jeener et Brachet, B6041 Gosselies, Belgium. [2]Department of Biochemistry, Trinity College, Dublin 2, Ireland. [3]Centre de Biophysique Moléculaire Numérique, Université de Gembloux, Belgium. [4]Structure et Fonction des Membranes Biologiques, Université Libre de Bruxelles, B1050 Brussels, Belgium. [5]Laboratory of Applied Genetics, IBMM, Université Libre de Bruxelles, B6041 Gosselies, Belgium.

*These authors contributed equally to this work.
†To whom correspondence should be addressed. E-mail: epays@ulb.ac.be

lytic domain, we compared apoL-I with the database of protein family motifs (Pfam). A marginal Pfam match ($E = 0.95$) suggested a similarity between the E77–W235 region and the pore-forming (pf) domain of bacterial colicins (*12–14*), e.g., V389–H592 of colicin A (colA) (fig. S1). We investigated whether this region might possess bactericidal activity similar to that of the colA pf domain by assessing the activity of a plasmid encoding the colA pf domain fused to the membrane signal peptide pelB (*13*, *14*), in which the colA sequence was replaced by different regions of apoL-I (Fig. 1A). The M60-L398 region of apoL-I, which corresponds to the secreted 39-kD form of apoL-I (*1*), could replace the colA pf domain in the assay, irrespective of whether pelB was present. Deletion of the entire C-terminal region from P304 did not affect bactericidal activity. A further deletion from A238 resulted in complete loss of activity, which was rescued by the presence of pelB. The region deleted (A238–L398) was not in

itself bactericidal even if pelB was added. Thus, the M60–W235 region was responsible for the bactericidal activity, and the C-terminal region P304–L398 was dispensable. The intervening region (A238–P304) was functionally analogous to pelB, although it did not act as a translocation signal peptide because it could not replace pelB in the colA pf domain assay. We will refer to this region as membrane-addressing (ma). Computational modeling of the ma sequence revealed two successive amphipatic α helices with a potential for hydrophobic interactions (fig. S2). Accordingly, the synthetic L248–A291 peptide exhibited affinity for lipids, as observed by measurement of the surface pressure of a DOPC (dioleoyl phosphatidyl choline) monolayer after injection of the peptide underneath the lipid phase. For an initial lipid pressure of ∼8 mN/m, an increase of 23 mN/m ± 2 mN/m was observed ($n = 3$), which is close to the effect of known lipid-interacting peptides (*15*).

The role of the different helices of the apoL-I bactericidal domain was assessed in *Escherichia coli* (Fig. 1A). As also observed for the colA pf domain (*14*), helices 1 to 3, 1 to 7, or 8 to 10 were inactive even when provided with pelB; however, when flanked by pelB, the hel4-10 region was active, although much less so than the full domain. A pelB-containing chimera associating helices 1 to 7 from colA and 8 to 10 from apoL-I was active, which could be important given the primary role of helices 8 and 9 in membrane insertion of the colicin pf domain (*13*, *14*).

The bactericidal domain of apoL-I functionally mimicked the colA pf domain, because both domains similarly impaired growth of *E. coli* provided that the pelB module was present (Fig. 1B), and in both cases the effect on the bacterial proton electrochemical gradient was the same as that produced when adding CCCP (carbonyl cyanide *m*-chlorophenylhydrazone), demonstrating that, like colicins, apoL-I depolarizes the bacterial membrane (Fig. 1C).

Reconstitution of the putative pf domain of apoL-I in planar lipid bilayer membranes allowed passage of steady-state currents that displayed small fluctuations between discrete levels, consistent with the presence of ion channels (Fig. 2, A and B). The magnitude of the unitary channel conductance ranged between 2.5 and 10 pS, which is similar to the conductance of the isolated pf domain of colicins (*16*). At equal KCL concentration ([KCl]) (300 mM) on both sides of the membrane, the current-voltage curve was linear between ±50 mV, whereas in asymmetric solution (300/590 mM), the reversal potential shifted toward positive voltages (Fig. 2C). The relative permeability of anions over cations was 3.2 ± 0.1.

This selectivity is opposite to that reported for planar lipid bilayer membranes (*17*), indicating that apoL-I increases the anion permeability of the membrane. Reconstitution of recombinant apoL-I into liposomes clearly altered the Cl⁻ permeability of the bilayer, as indicated by the large influx of $^{36}$Cl⁻ observed in the presence of apoL-I. This result was not observed with apoL-I lacking the putative pf domain (Fig. 2D). The influx of $^{36}$Cl⁻ was higher at pH 5 than at pH 7, and it was insensitive to the anion-channel inhibitor DIDS (4,4-diisothiocyanatostilbene-2,2-disulfonic acid) (Fig. 2D).

Several apoL-I recombinant proteins were reconstituted into apoL-I–depleted normal human serum (NHS) (*6*) (fig. S3) and assayed for trypanolytic activity using NHS-sensitive (SRA⁻) and NHS-resistant (SRA⁺) *T. b. rhodesiense* clones. Recombinant apoL-I induced lysis of sensitive parasites only, with kinetics similar to that of NHS levels containing equivalent amounts of native apoL-I (Fig. 3A). The pf and ma domains of apoL-I were both required for trypanolysis, and the former domain could not be replaced by the colA pf domain in this assay (Fig. 3A). ApoL-I is normally associated with HDLs (*1*), and this association could allow rapid uptake of the toxin through receptor-mediated endocytosis of HDLs (*7–10*). Accordingly, the simple addition of recombinant apol-I to depleted serum without reconstitution delayed the lysis (Fig. 3A). Converting the negatively charged helix of the ma domain into a positive helix (D249K/E253K/E256K) (fig. S2) resulted in a total loss of trypanolytic activity equivalent to deletion of this domain (Fig. 3A). This mutant was also inactive in *E. coli* but recovered full activity when provided with the bacterial signal peptide (Fig. 1A). Thus, in trypanosomes, the ma domain probably targets apoL-I to a membrane, presumably the lysosomal membrane, because apoL-I localizes in this compartment (*6*).

Trypanosome lysis was analyzed in immobilized live cells. NHS or recombinant apoL-I, but not fetal calf serum (FCS) or the inactive D249K/E253K/E256K apoL-I mutant, caused swelling of the lysosome (Fig. 4A). The lysosome appeared empty and progressively occupied most of the cell body (Fig. 4B). These observations are consistent with osmotic swelling due to inward movement of an osmotically active species. Cl⁻ influx might be responsible because the cytoplasmic [Cl⁻] is unusually high in trypanosomes (106 mM) (*18*) and the apoL-I pf domain is selective for anions. Lysosomal swelling and trypanolysis by NHS were both stopped when trypanosomes were transferred to a medium in which
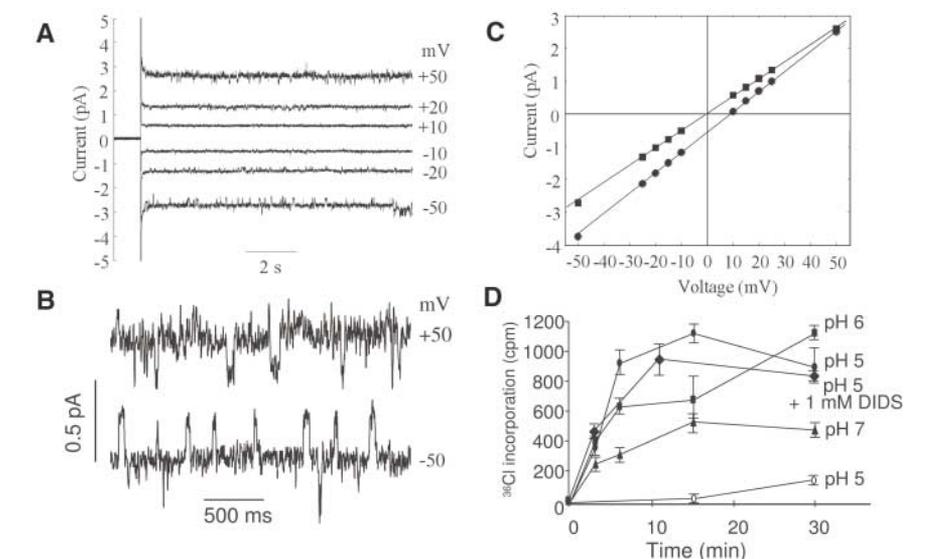
Cl⁻ was replaced with gluconate (Fig. 3B). Lysis still occurred when the trypanosomes were transferred to a medium with Cl⁻ or to a medium with Na⁺ replaced by



**Fig. 2.** Ion currents generated by apoL-I in lipid membranes. (**A** to **C**) Current traces recorded with planar lipid bilayer membranes containing the apoL-I pf domain. (**A**) Results at different voltages (mV) in 300 mM KCl. (**B**) Time scale–expanded current traces showing small current fluctuations between discrete levels, indicating channel gating. (**C**) Current-voltage curve in a symmetric 300 mM KCl (■) and in an asymmetric trans/cis 300/590 mM KCl (●). (**D**) $^{36}$Cl flux into liposomes reconstituted with apol-I. The Cl⁻ incorporation was compared after insertion of the full apoL-I (filled symbols) or its version depleted of the pf domain (open symbols).
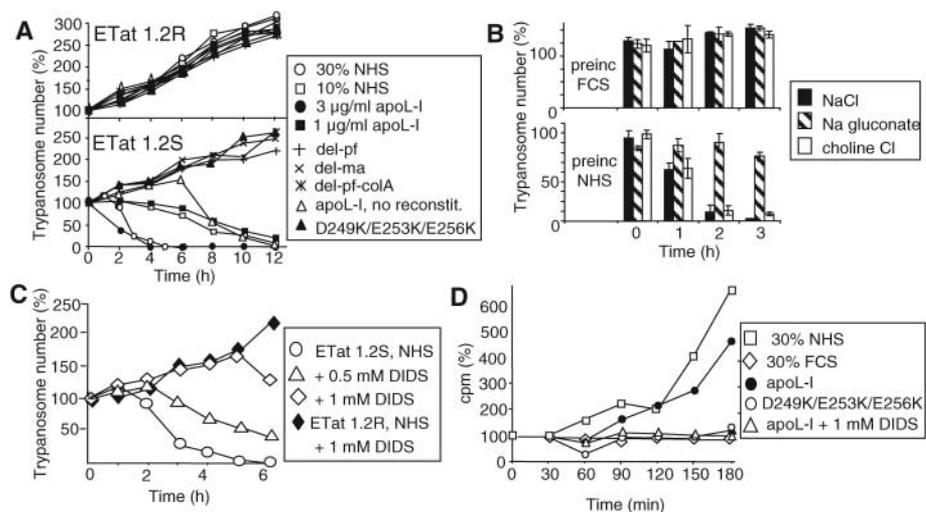


**Fig. 3.** Trypanosome lytic activity of apoL-I derivatives. (**A**) Effects on *T. b. rhodesiense* clones ETat 1.2S and ETat 1.2R (NHS-sensitive and NHS-resistant, respectively) of either NHS or serum reconstituted with the following recombinant proteins (3 μg/ml, unless stated otherwise): apoL-I, E28-L398; del-pf, deletion of the pf domain; del-ma, deletion of the membrane-addressing domain; del-pf-colA, replacement of the pf domain by that of colA; D249K/E253K/E256K, mutant of the ma domain. Assays were also conducted without proper serum reconstitution. 100%, $5 \times 10^5$ trypanosomes/ml. (**B**) Evidence for the involvement of Cl⁻ in trypanolysis by NHS. After incubation for 1 hour at 37°C in either 30% NHS or 30% FCS, the trypanosomes were centrifuged and then incubated at 37°C in 10 mM glucose, 1 mM hypoxanthine, catalase (50 μg/ml), 25 mM Hepes (pH 7.4) containing 10% FCS, and either 100 mM NaCl (■), 100 mM Na gluconate (■), or 100 mM choline Cl (□). (**C**) Effect of the Cl⁻ channel blocker DIDS on ETat 1.2S or ETat 1.2R trypanosomes incubated with 30% NHS. (**D**) Effect of recombinant apoL-I derivatives (3 μg/ml) and NHS or FCS (30%) on the amount of intracellular $^{36}$Cl. About 50% of the cells were still alive, but swollen, after 180 min in either NHS or apoL-I. 100%, ~200 cpm.

choline, although after preincubation with FCS, none of these conditions affected the trypanosomes (Fig. 3B). Furthermore, the anion blocker DIDS, which inhibits Cl⁻

channels of *T. brucei* (*19*), led to a substantial delay in lysis by NHS (Fig. 3C). At the same concentrations of DIDS, NHS-resistant parasites grew normally, indicating that the effect of DIDS on trypanolysis was specific (Fig. 3C). Finally, incubation of trypanosomes with NHS or recombinant apoL-I, but not FCS or the inactive D249K/E253K/E256K mutant, led to a DIDS-sensitive influx and accumulation of extracellular Cl⁻ in the cells (Fig. 3D). Thus, apoL-I triggered both the influx of Cl⁻ and the swelling of the lysosome. Because preventing the Cl⁻ flux by either removal of ions or blocking the ion channels inhibited the swelling, apoL-I must induce the ionic flux first.

The apoL-I–mediated effect was likely to involve the lysosomal membrane, because in trypanosomes apoL-I tightly colocalizes with the lysosomal membrane marker p67 (*6*). Indeed, in NHS-sensitive trypanosomes, apoL-I was concentrated at the periphery of the swollen lysosome (Fig. 4C). Moreover, the NHS-induced influx of Cl⁻ was linked to the specific loss of lysosomal fluorescence by the membrane-potential

probe RH414 (*20*) (Fig. 4D). Imaging analysis indicated a rapid 200-fold decrease in lysosomal-associated fluorescence but no major change in mitochondrial-associated fluorescence (Fig. 4D). Despite its clear inhibitory effect on lysosome swelling by NHS, DIDS did not affect the NHS-induced change in lysosomal RH414 fluorescence (Fig. 4D). Moreover, DIDS did not affect the pf activity of apoL-I, but it clearly inhibited the NHS/apoL-I–mediated influx of extracellular ³⁶Cl⁻ (Fig. 3D). Thus, the inhibition by DIDS of trypanosome swelling and lysis by NHS was probably due to blocking of Cl⁻ entry into the cell. The most likely explanation is that the apoL-I–mediated influx of Cl⁻ from the cytoplasm to the lysosome causes a change in cytoplasmic [Cl⁻] that in turn causes a compensatory movement of extracellular Cl⁻ across the plasma membrane through DIDS-sensitive channels (*19*) (fig. S4). The internal pressure resulting from the continuous enlargement of the lysosome presumably compromises the physical integrity of the plasma membrane, explaining the fraying of the surface coat and leakage of ions that precede lysis (*21*).

These data contradict the model of lysis through disruption of the lysosomal membrane (*8, 11*).

The Bcl-2 family is the only known example of eukaryotic proteins bearing a colicin-like pf domain (*22*), but the role of this domain is unclear (*23*). The pf domain is conserved within the human apoL family, most members of which encode intracellular proteins (*2, 3*). Thus, the original function of apoLs might be the formation of pores in intracellular membranes. In humans, the appearance of an apoL version with a signal peptide created a new component of innate immunity endowed with antimicrobial activity.

### References and Notes

1. P. N. Duchateau *et al.*, *J. Biol. Chem.* **272**, 25576 (1997).
2. N. M. Page *et al.*, *Genomics* **74**, 71 (2001).
3. P. N. Duchateau *et al.*, *J. Lipid Res.* **42**, 620 (2001).
4. H. Monajemi *et al.*, *Genomics* **79**, 539 (2002).
5. P. Poelvoorde *et al.*, *Mol. Biochem. Parasitol.* **134**, 155 (2004).
6. L. Vanhamme *et al.*, *Nature* **422**, 83 (2003).
7. L. Vanhamme, E. Pays, *Int. J. Parasitol.* **34**, 887 (2004).
8. K. M. Hager *et al.*, *J. Cell Biol.* **126**, 155 (1994).
9. M. R. Rifkin, *J. Lipid Res.* **32**, 639 (1991).
10. H. P. Green *et al.*, *J. Biol. Chem.* **278**, 422 (2003).
11. M. Shimamura, K. M. Hager, S. L. Hajduk, *Mol. Biochem. Parasitol.* **115**, 227 (2001).
12. J. Morlon *et al.*, *J. Mol. Biol.* **170**, 271 (1983).
13. D. Duché, *Biochimie* **84**, 455 (2002).
14. A. Nardi *et al.*, *J. Mol. Biol.* **307**, 1293 (2001).
15. R. Maget-Dana, *Biochim. Biophys. Acta* **1462**, 109 (1999).
16. P. K. Kienker *et al.*, *J. Gen. Physiol.* **122**, 161 (2003).
17. B. Fuks, F. Homblé, *Biophys. J.* **66**, 1404 (1994).
18. D. P. Nolan, H. P. Voorheis, *Eur. J. Biochem.* **267**, 4615 (2000).
19. N. Vanderheyden, J. Wong, R. Docampo, *Biochem. J.* **346**, 53 (2000).
20. A. Grinvald *et al.*, *Nature* **308**, 848 (1984).
21. M. R. Rifkin, *Exp. Parasitol.* **58**, 81 (1984).
22. S. W. Muchmore *et al.*, *Nature* **381**, 335 (1996).
23. Y. Lazebnik, *Curr. Biol.* **11**, R767 (2001).
24. We thank D. Duché (Marseille) for the gift of plasmids; K. Zouaoui Boudjeltia and M. Vanhaeverbeek (Vésale Charleroi) for help in collecting NHS; G. Vansanten, F. Delfosse, E. Dupont, C. Felu, and M. Magi for assistance; and G. Vandenbussche and C. Miller for advice. This work was supported by the Belgian National Fund for Scientific Research (FNRS, FRSM, and Crédit aux Chercheurs), the United Nations Development Program/World Bank/World Health Organization Special Programme for Research and Training in Tropical Diseases, and the Communauté Française de Belgique–Action de Recherches Concertées and the Interuniversity Attraction Poles Programme–Belgian Science Policy. F.H. and R.B. are Research Directors, L.V. and L.L. are Research Associates, and B.V. is a Research Fellow, all at the FNRS; D.P.N. is a senior fellow of the Wellcome Trust.
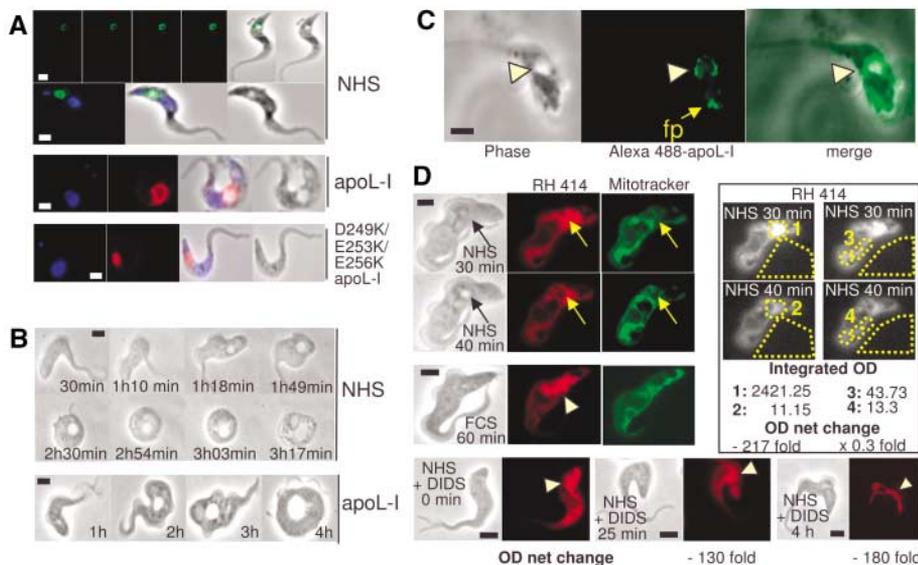
**Fig. 4.** Cellular effects of apoL-I. (**A**) Localization of the lysosomal membrane protein p67, detected by Alexa 488 (green)– or Alexa 594 (red)–coupled antibodies in trypanosomes incubated for 30 min at 33°C with 20% NHS (two upper rows) or with recombinant wild-type apoL-I (2 μg/ml) (third row) or D249K/E253K/E256K mutant apoL-I (bottom row). Top row: serial sections by confocal microscopy; other panels: epifluorescence microscopy [large and small blue dots, DAPI (4′,6′-diamidino-2-phenylindole)–stained nucleus and kinetoplast, respectively]. (**B**) Cellular changes induced in immobilized live trypanosomes at 33°C, by 10% NHS or serum reconstituted with recombinant apoL-I (1 μg/ml). Higher NHS concentrations and/or higher temperatures resulted in acceleration of the kinetics of lysis. (**C**) Localization of Alexa 488-apoL-I after incubation of ETat 1.2S parasites for 2 hours at 37°C (fp, flagellar pocket). (**D**) Effect of 30% NHS, 30% FCS, or 30% NHS + DIDS (1 mg/ml) on in vivo lysosomal fluorescence at 33°C by the membrane-potential probe RH414. Similar results were obtained with the RH414-like endolysosomal probe FM 4-64 (not shown). The arrows point to the lysosomal region, identified by the empty vacuole appearing between 30 and 40 min after addition of NHS. Arrowheads point to the corresponding region in trypanosomes where the lysosome does not swell. The mitotracker stains the mitochondrion. The panels at the right show the surfaces where the intensity of fluorescence was measured (1 to 4), using the respective control area. In all panels, the bar represents 2 μm.